FEBS Letters 589 (2015) 1257–1265

FEBS Letters

journal homepage: www.FEBSLetters.org

Mesenchymal-stem-cell-derived exosomes accelerate skeletal muscle regeneration

Yoshihiro Nakamura [a,*,1], Shigeru Miyaki [a,b,1], Hiroyuki Ishitobi [b], Sho Matsuyama [a], Tomoyuki Nakasa [a], Naosuke Kamei [a,b], Takayuki Akimoto [c], Yukihito Higashi [b], Mitsuo Ochi [a]

[a] Department of Orthopedic Surgery, Hiroshima University, Hiroshima, Japan
[b] Department of Regenerative Medicine, Hiroshima University Hospital, Hiroshima, Japan
[c] Division of Regenerative Medical Engineering, Center for Disease Biology and Integrative Medicine, Graduate School of Medicine, University of Tokyo, Tokyo, Japan

ARTICLE INFO

Article history:
Received 11 March 2015
Accepted 26 March 2015
Available online 8 April 2015

Edited by Berend Wieringa

Keywords:
Exosome
Mesenchymal stem cell
Skeletal muscle
Regeneration
MicroRNA

ABSTRACT

Mesenchymal stem cell (MSC) transplantation is used for treatment of many diseases. The paracrine role of MSCs in tissue regeneration is attracting particular attention. We investigate the role of MSC exosomes in skeletal muscle regeneration. MSC exosomes promote myogenesis and angiogenesis in vitro, and muscle regeneration in an in vivo model of muscle injury. Although MSC exosomes had low concentrations of muscle-repair-related cytokines, a number of repair-related miRNAs were identified. This study suggests that the MSC-derived exosomes promote muscle regeneration by enhancing myogenesis and angiogenesis, which is at least in part mediated by miRNAs such as miR-494.

1. Introduction

Mesenchymal stem cells (MSCs) differentiate into many cell types, including osteoblasts, chondrocytes, adipocytes, and myoblasts [1]. There is considerable interest in the clinical application of MSCs for the treatment of many diseases. However, several studies have reported transplanted MSCs show poor engraftment efficiency and have not always shown tissue-specific differentiation [1–3]. Although the transplantation of MSCs promoted the regeneration of skeletal muscle in a rat injury model, the cells did not differentiate into skeletal myofibers [4]. Our previous study indicated MSCs contribute to the regeneration of skeletal muscle by mechanisms other than myogenic differentiation [4]. Therefore, the paracrine role of MSCs is attracting attention to explain their effect on tissue regeneration. Many reports have demonstrated that the paracrine activity of MSCs has a therapeutic effect on a variety of diseases, tissue injury in myocardium [5], kidney [6], liver [7], and lung [8].

Recently, extracellular vesicles, including exosomes, have attracted attention as new players in cell-to-cell communication. Exosomes are vesicle of the multivesicular body, a complex intracellular organelle involved in endocytosis. The diameter of exosomes is typically 30–200 nm. After multivesicular bodies fuse with the plasma membrane, exosomes are released from the cells into the extracellular environment. Exosomes contain messenger RNA (mRNA) and microRNA (miRNA) as well as proteins, and the functional RNAs can be transferred from one cell to another by the exosome [9,10]. The properties of exosomes reflect the specialized properties of their original cells and the environment. In fact, recent studies have shown that microvesicles derived from MSCs have regenerative functions in several tissues, including kidney, heart, nervous tissues, liver, and lung [11–20]. We hypothesized that exosomes from MSCs exert a novel paracrine effect on skeletal muscle repair during MSC transplantation, in addition to their secretion of cytokines, chemokines, or growth factors.

Author contributions: Y.N.: the conception and design of the study, acquisition of data, analysis and interpretation of data, manuscript writing; S.M.: the conception and design of the study, acquisition of data, analysis and interpretation of data, manuscript writing; H.I.: acquisition of data, analysis and interpretation of data; S.M.: acquisition of data; T.N.: analysis and interpretation of data; N.K.; analysis and interpretation of data; T.A.: acquisition of data, analysis and interpretation of data; Y.H.: analysis and interpretation of data; M.O.: final approval of the version to be submitted.

* Corresponding author at: Department of Orthopedic Surgery, Hiroshima University, 1-2-3 Kasumi, Hiroshima 734-8551, Japan. Fax: +81 82 257 5234.
E-mail address: nakamurayoshihiro0419@gmail.com (Y. Nakamura).
[1] Yoshihiro Nakamura and Shigeru Miyaki contributed equally to this work.

http://dx.doi.org/10.1016/j.febslet.2015.03.031
0014-5793/

2. Materials and methods

2.1. Culture of human MSCs and synovial fibroblasts

Four independent human bone-marrow-derived MSCs were obtained from Lonza (Basel, Switzerland) and cultured in MSC growth medium (Lonza). MSCs at passage 4–5 were used in the experiments. Human synovial fibroblasts (SFB) were isolated and cultured as described previously [21].

2.2. Preparation of conditioned medium and isolation of exosomes

MSCs were seeded at 1.0×10^5/well in a six-well plate with Dulbecco's modified Eagle's medium (DMEM; Life Technologies, USA) containing 10% fetal bovine serum (FBS; Life Technologies) and 1% antibiotic–antimycotic solution (Nacalai Tesque, Japan). The cells were washed with serum-free DMEM and cultured with 2 ml/well serum-free DMEM for 48 h at 37 °C under 5% CO_2. The conditioned media (MSC-CM) were collected and centrifuged for 15 min at 2380×*g*, and then further ultracentrifuged for 70 min at 110000×*g* (Optima TL ultracentrifuge, Beckman Coulter, USA). The supernatants were collected, and were concentrated using Amicon Ultra-2 centrifugal filters (Millipore, USA) as exosome-depleted conditioned media (MSC-CM (exo−)). To isolate the exosomes (MSC-exosomes), the pellets were washed in Phosphate-buffered saline (PBS) and a second ultracentrifugation was performed for 70 min at 110000×*g*. The exosomes isolated from the same volumes of culture medium from the same numbers of cells were resuspended in PBS or DMEM for use as fresh preparation.

2.3. Immunoblotting of exosome markers

The exosome marker proteins from the cells, the exosomes, and the MSC-CM (exo−) were detected by immunoblotting. Anti-flotillin-1 antibody (610820; diluted 1:500; BD Biosciences, USA), purified mouse anti-human CD9 antibody (diluted 1:200; BD Bioscience), and anti-CD81 antibody (sc-7637; diluted 1:200; Santa Cruz Biotechnology, USA) were used as primary antibodies. Horseradish peroxidase (HRP)-conjugated IgG antibody (sc-2005, sc-2030; Santa Cruz Biotechnology) was used as the secondary antibody.

2.4. Exosome size analysis

Exosomes isolated by ultracentrifugation were resuspended in 100 mM KCl and 40 mM HEPES. The sizes and numbers of MSC particles were measured on an Izon qNano system with tunable resistive pulse sensor (TRPS) technology (Izon Science, New Zealand), as previously reported [22].

2.5. Culture of C2C12 cells for myogenesis

The mouse C2C12 myoblast cell line (American Type Culture Collection) was cultured in DMEM containing 10% FBS. The C2C12 cells were seeded at 2.0×10^4/well in a 24-well plate. To examine the effects of exosomes on myogenic differentiation, the medium was changed to DMEM, MSC-conditioned medium (MSC-CM), MSC-exosome suspension in DMEM (MSC-exosome), or exosome-depleted MSC-conditioned medium (MSC-CM (exo−)) containing 2% horse serum (Life Technologies). The cells were incubated at 37 °C under 5% CO_2 for 4 days.

2.6. Quantitative real-time PCR

Total RNA was extracted from them using TRIzol Reagent (Invitrogen). Complementary DNA (cDNA) was synthesized using 1 μg of total RNA with the SuperScript VILO cDNA Synthesis Kit (Invitrogen). A real-time PCR assay was performed using TaqMan Gene Expression Assay probes (Life Technologies) to amplify the MyoD gene (Myod1; Mm00440387_m1) and Myogenin gene (Myog; Mm00446194_m1). The glyceraldehyde-phosphate dehydrogenase gene (Gapdh; Mm99999915_g1) was used as the internal control to normalize the sample differences. The ΔΔCt method was used to analyze the real-time PCR data.

2.7. Immunocytochemical analysis of the myosin heavy chain

The C2C12 cells were fixed with 4% paraformaldehyde after 4 days in differentiation medium. The cells were incubated overnight at 4 °C with primary mouse anti-F59 (myosin heavy chain) antibody (Hybridoma Bank, USA). They were incubated with secondary antibody, Alexa-Fluor-568-conjugated goat anti-mouse IgG antibody (Molecular Probes; Invitrogen) for 1 h at room temperature. 4′,6,-Diamidino-2-phenylindole (DAPI; Dojindo Laboratories, Japan) solution was applied for 5 min to stain the

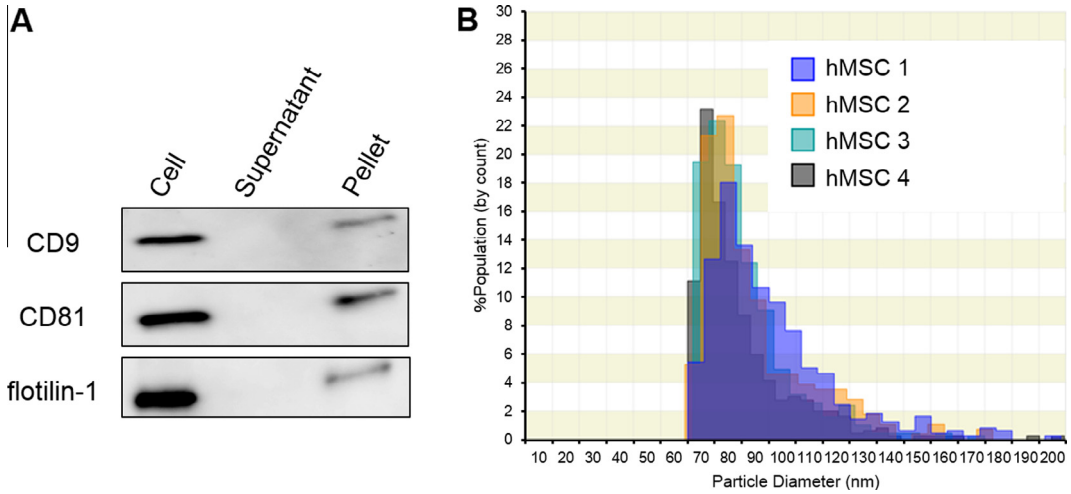

Fig. 1. Exosome isolation from mesenchymal-stem-cell-derived conditioned medium by ultracentrifugation. (A) Immunoblotting of the ultracentrifugation pellet and supernatant for exosomal surface proteins: CD9, CD81, and flotillin-1. (B) The size distribution of the particles in the pellet was measured with the qNano system. Abbreviations: hMSC, human mesenchymal stem cell.

nuclei. Three random microscopic areas in each well were selected at ×200 magnification. The total numbers of nuclei were counted to evaluate cell proliferation, and the fusion index (ratio of the nuclei in myotubes to all nuclei) was calculated to evaluate myogenic differentiation.

2.8. Culture of HUVECs and migration assay

Human umbilical-vein endothelial cells (HUVECs) were purchased from Lonza and were maintained in EBM-2 (Lonza) supplemented with 10% FBS and growth factors (BulletKit, Lonza). HUVECs suspended in 500 µl of serum-free DMEM were seeded at 2×10^4/well to the 24-well upper chamber of a cell culture insert with an 8.0 µm pore polyethylene terephthalate track-etched membrane (BD Falcon Cell Culture inserts; BD Biosciences, Canada). The chambers were placed in 24-well plates. DMEM, MSC-CM, MSC-exosomes, or MSC-CM (exo−) was added to the bottom well of the multiwall insert assembly in 750 µl of serum-free medium. After incubation for 4 h, the lower side of the filter was fixed with 4% paraformaldehyde. The migrated cells were quantified as the number of cell nuclei stained with DAPI.

2.9. Tube formation assay

An angiogenesis assay kit (Kurabo, Japan) was used for the tube formation assay, according to the manufacturer's instructions. HUVECs were cultured with DMEM, MSC-CM, MSC-exosomes, or MSC-CM (exo−). After 4 days, the medium was replaced with the same conditioned medium. After 8 days, the cells were fixed with ethanol and the newly formed tubes were visualized with a tubule staining kit (Kurabo). Micrographs were taken at ×40 magnification in all fields per well and image fusion was performed. The total

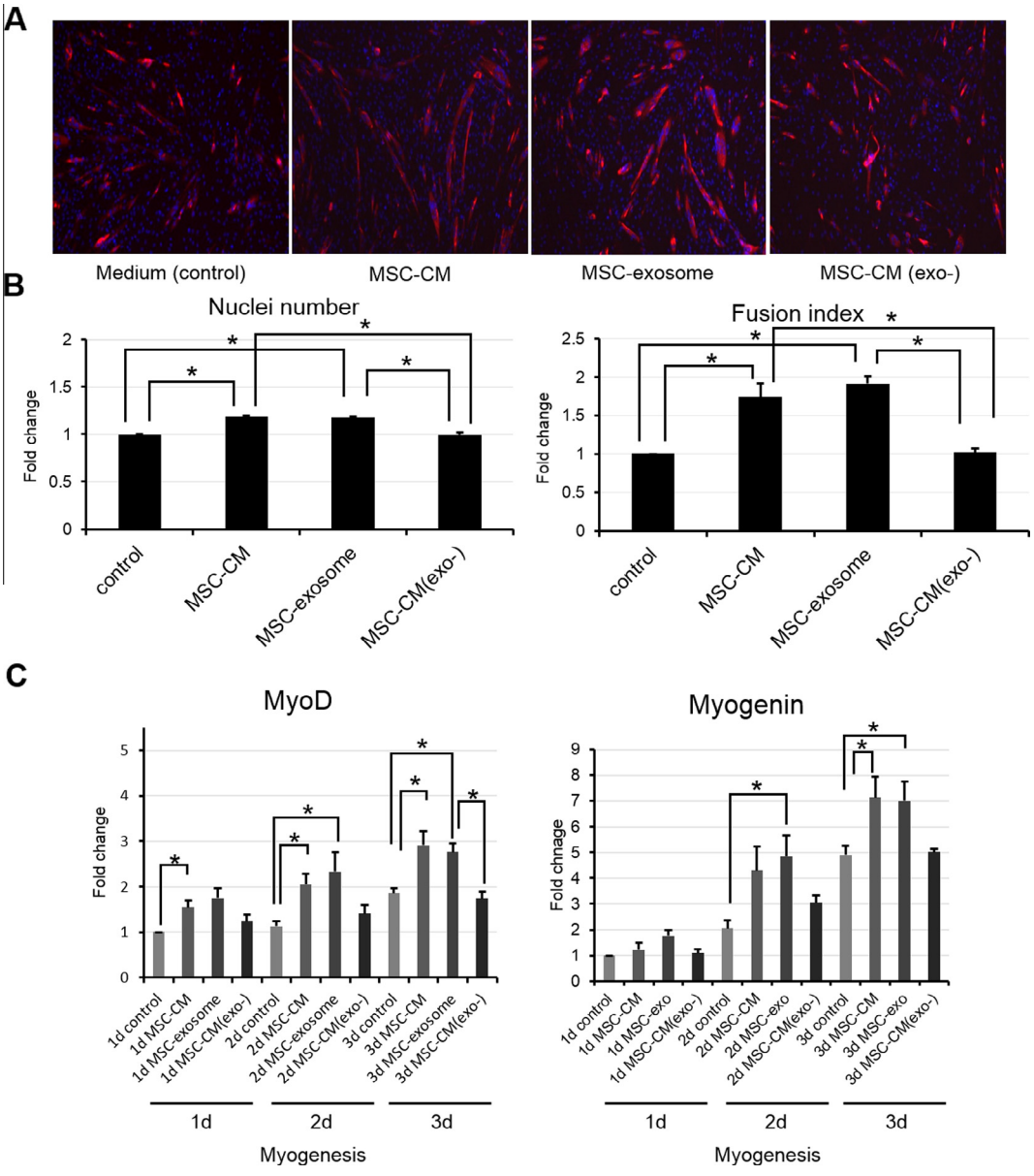

Fig. 2. Effects of MSC-exosomes on the differentiation of C2C12 cells. (A) Immunocytochemical analysis of myosin heavy chain 4 days after the induction of differentiation. Myotubes are stained red and nuclei are stained blue. Original magnification, ×200. (B) Total nuclei numbers indicate myoblast proliferation. The fusion index indicates the differentiation of C2C12 cells. (C) Real-time PCR analysis of the marker genes of myogenesis, *Myod1* and *Myog*, in C2C12 cells 1, 2, and 3 days after the induction of differentiation. All data were calculated as means ± S.E. ($n = 5$). Statistical analysis was performed with the Steel–Dwass test. $^*P < 0.05$ versus control or MSC-CM (exo−). Abbreviations: control, DMEM; MSC-CM, mesenchymal-stem-cell-derived conditioned medium; MSC-CM (exo−), mesenchymal-stem-cell-derived exosome-depleted conditioned medium; MSC-exosomes, mesenchymal-stem-cell-derived exosome suspension in DMEM.

tube lengths in the full visual field of each well were measured under a digital microscope BZ-9000 (Keyence, Japan).

2.10. Mouse model of cardiotoxin-induced muscle injury and local injection of exosomes

This study was reviewed and approved by the Ethics Committee for Experimental Animals of Hiroshima University, and all animals were treated according to the guidelines of the Institutional Animal Care and Use Committee. Eight-week-old male C57BL/6 mice (five per group) were anesthetized with isoflurane. One hundred microliter of 10 μM cardiotoxin (Sigma, USA) in PBS was injected into the right side of the belly of the tibialis anterior muscle. PBS (50 μl) or MSC-exosomes resuspended in PBS (50 μl) was injected into right side of the belly of the tibialis anterior muscle 1, 3, and 5 days after muscle injury.

2.11. Histological evaluation

Seven days after muscle injury, the tibialis anterior muscles of each group were harvested and mounted in Tissue Freezing Medium (Triangle Biomedical Sciences, USA), quickly frozen in liquid nitrogen, and stored at −80 °C. The frozen muscles were cut into 6 μm sections in the axial plane and air-dried. To evaluate muscle regeneration, each sample was stained with hematoxylin and eosin. Centronucleated myofibers are recognized as regenerated myofibers. Conversely, preexisting myofibers are identified by the positions of their nuclei at the cell periphery. At ×200 magnification of the axial sections, the diameter and the total number of centronucleated myofibers were measured in four random fields. To evaluate the fibrotic area, each sample was stained with Masson trichrome. The average areas of fibrosis in the axial sections were determined under a digital microscope (BZ-9000, Keyence).

2.12. Immunofluorescence analysis to evaluate capillary density

Tissue sections were stained immediately with the following primary antibodies: anti-dystrophin antibody (D8043; Sigma–Aldrich) and anti-mouse CD31 antibody, a marker of endothelial cells (MCA2388; AbD Serotec). The secondary antibodies were Alexa-Fluor-549-conjugated anti-mouse IgG1 (for dystrophin) and DyLight-488-conjugated anti-rat IgG (for CD31) (Jackson ImmunoResearch). Four randomly selected areas in the axial sections were evaluated at ×200 magnification.

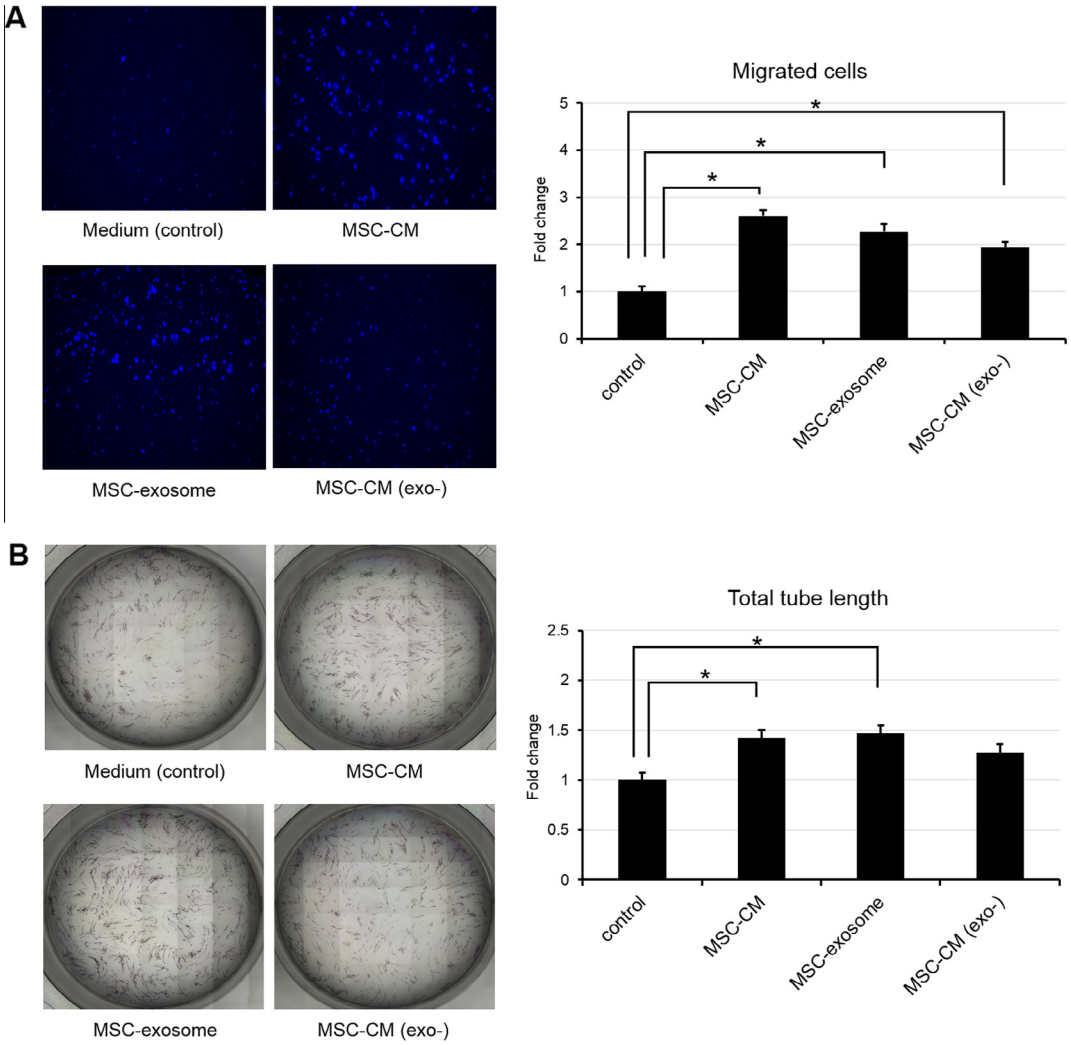

Fig. 3. Effects of MSC-exosomes on the angiogenic activity on HUVECs. (A) Migration assay using HUVECs. The numbers of migrated cells were counted. Nuclei of the migrated cells are stained blue. Original magnification, ×100. (B) In the tube formation assay, the tube lengths of HUVECs that had been cocultured with human fibroblasts for 8 days were measured. Original magnification, ×200. Image fusion was performed. All data were calculated as means ± S.E. (n = 5). Statistical analysis was performed with the Steel–Dwass test. *P < 0.05 versus control or MSC-CM (exo−).

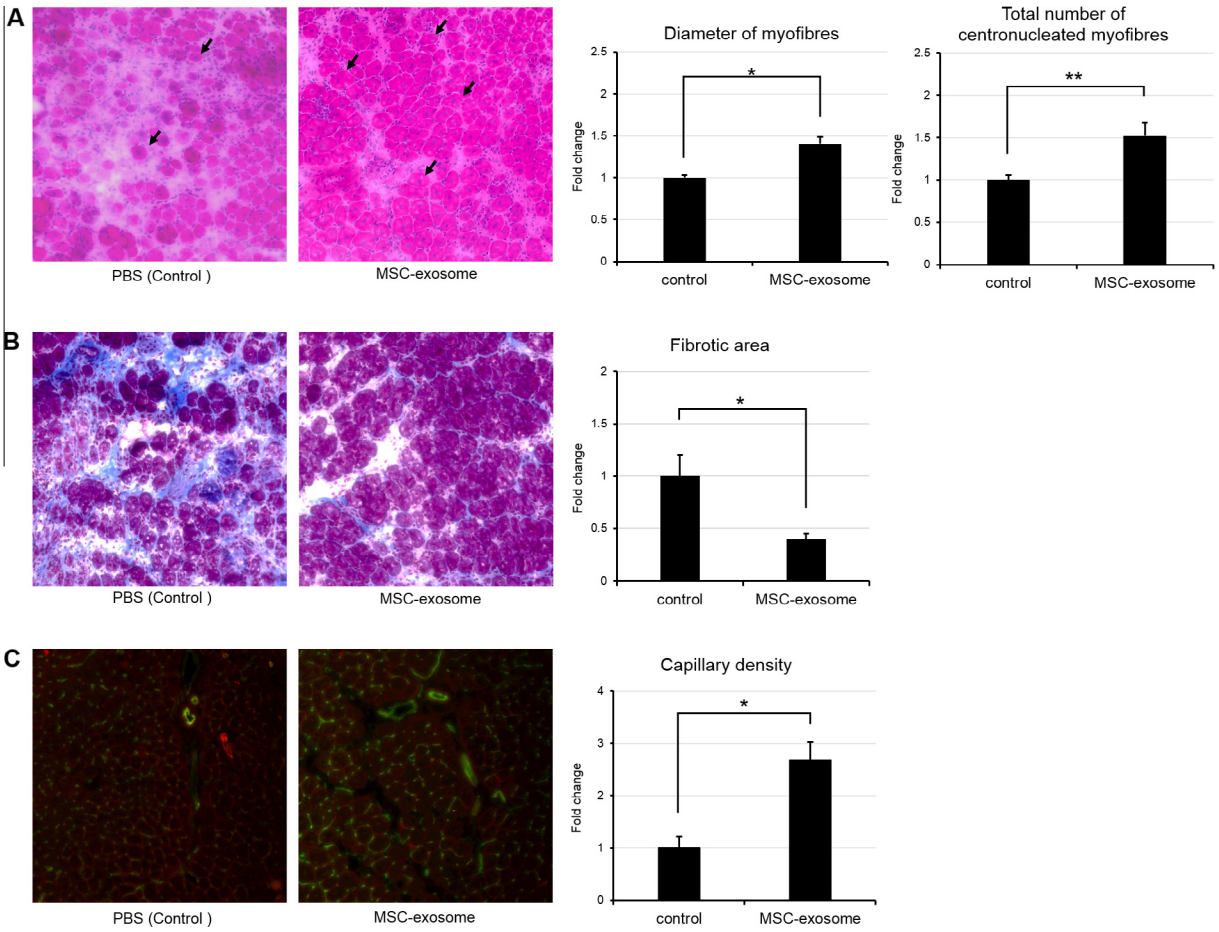

Fig. 4. Improved tissue regeneration in mouse tibialis anterior muscle injury model following injection of MSC-exosomes. The effects of injection with mesenchymal-stem-cell-derived exosomes were compared with the effects of phosphate-buffered saline injection in the cardiotoxin induced muscle injury model. (A) Representative histological evaluation of regeneration, with hematoxylin and eosin staining. (B) Representative histological evaluation of fibrosis with Masson trichrome staining. The fibrotic area is stained blue. (C) Representative histological evaluation of capillary density, with immunofluorescent staining for CD31. Vascular endothelial cells are stained green. Original magnification, ×200. All data were calculated as means ± S.E. ($n = 5$). Statistical analysis was performed with the Mann–Whitney test. $^{*}P < 0.05$ versus control.

2.13. Cytokine/growth factor assay

The insulin-like growth factor 1 (IGF-1) levels in MSC-CM, MSC-exosomes, and MSC-CM (exo−) were measured with an enzyme-linked immunosorbent assay (ELISA) using a Quantikine Human IGF-1 ELISA (R&D Systems USA). Vascular endothelial growth factor (VEGF), interleukin 6 (IL-6), fibroblast growth factor 2 (FGF2), granulocyte colony-stimulating factor (GCSF), and platelet-derived growth factor-BB (PDGF-BB) levels in the MSC-CM, MSC-exosomes, and MSC-CM (exo−) were quantified using the Bio-Plex Multiplex suspension assay system (Bio-Rad Laboratories).

2.14. Nanostring nCounter miRNA analysis

MSC-exosomes were isolated from the total conditioned medium (15 ml) on four independent MSCs seeded at 2.5×10^6 cells/150 × 25 mm plate. SFB-derived exosomes (SFB-exosomes) were also isolated under the same conditions as MSC-exosomes. The small RNAs were purified from the MSC, MSC-exosomes, MSC-CM (exo−), and SFB-exosomes using the mirVana miRNA Isolation Kit (Life Technologies). Purified small RNAs were enriched using evaporator. The concentrations and quality of the small RNAs from the same volumes of culture medium for the same numbers of cells were determined with the BioAnalyzer 2100 (Agilent Technologies, USA), and at least 5 ng of small RNA was used as the input for the nCounter Human miRNA Expression Assay Kit (NanoString Technologies, USA). The miRNA expression profiles were analyzed according to manufacturer's instructions.

2.15. Transfection

C2C12 cells or HUVECs were transfected with miR-494 using Lipofectamine RNAiMax Reagent (Invitrogen) using 10 or 50 nM of miR-494 or control (siRNA negative control; siNega #1, Ambion, USA). The sequences of the double-stranded miR-494 were: (sense) 5′-AGGUUGUCCGUGUUGUCUUCUC-3′ and (antisense) 5′-UGAAACAUACACGGGAAACCUC-3′ (Hokkaido System Sciences, Japan). C2C12 cells were induced to undergo myogenic differentiation 24 h after transfection. The HUVECs were harvested and used for migration assays.

2.16. Statistical analysis

The results are expressed as means ± S.E. The data were analyzed with the Steel–Dwass test or the Mann–Whitney test. P values <0.05 were considered to be statistically significant.

3. Results and discussion

3.1. Exosomes from MSCs

The exosome markers CD9, CD81, and flotillin-1 in immunoblotting were present in the pellets (MSC-exosomes) after

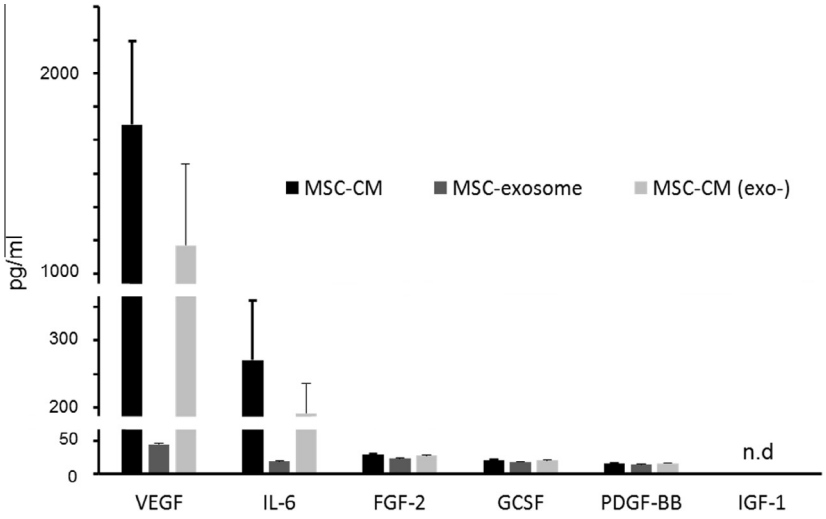

Fig. 5. Cytokines, growth factors in MSC-exosomes. The concentrations of the muscle-repair-related cytokines in exosomes were measured in MSC-CM, MSC-exosomes, and MSC-CM (exo−) using ELISAs or Bio-Plex assays. Abbreviations: N.D., not detected. $N = 4$ independent hMSC.

Table 1
Top-20 microRNAs.

	miRNAs[a] in MSC-exosomes[b]	miRNAs in MSC[c]	miRNAs in MSC-CM (exo−)[d]
1	**hsa-miR-21-5p**	hsa-miR-125b-5p	**hsa-miR-4454**
2	**hsa-miR-4454**	hsa-let-7a-5p	**hsa-miR-125b-5p**
3	hsa-miR-378e	hsa-miR-21-5p	**hsa-let-7a-5p**
4	**hsa-miR-125b-5p**	hsa-let-7b-5p	**hsa-miR-21-5p**
5	hsa-miR-495	hsa-miR-4454	hsa-miR-720
6	hsa-miR-1183	hsa-miR-29b-3p	hsa-miR-4286
7	hsa-miR-598	hsa-miR-23a-3p	hsa-miR-4488
8	hsa-miR-25-3p	hsa-miR-199a-3p + 199b-3p	**hsa-let-7b-5p**
9	hsa-miR-570-3p	hsa-let-7i-5p	**hsa-miR-23a-3p**
10	hsa-miR-720	hsa-miR-100-5p	**hsa-miR-199a-3p + 199b-3p**
11	hsa-miR-302d-3p	hsa-miR-29a-3p	hsa-miR-378e
12	hsa-miR-23a-3p	hsa-let-7g-5p	**hsa-miR-145-5p**
13	hsa-miR-548al	hsa-miR-221-3p	hsa-miR-4516
14	hsa-miR-579	hsa-miR-15a-5p	**hsa-miR-100-5p**
15	hsa-miR-630	hsa-miR-143-3p	**hsa-let-7g-5p**
16	hsa-miR-888-5p	hsa-miR-16-5p	**hsa-miR-4454**
17	hsa-miR-155-5p	hsa-miR-22-3p	**hsa-miR-221-3p**
18	hsa-miR-761	hsa-miR-145-5p	**hsa-let-7i-5p**
19	hsa-miR-375	hsa-miR-27b-3p	hsa-miR-1260a
20	hsa-miR-548aa	hsa-miR-125a-5p	hsa-miR-630

Listed are the top 20 miRNAs according to their expression levels in MSC-exosomes, MSC, and MSC-CM (exo−) according to the NanoString miRNA profile ($n = 4$). miRNAs in bold font were expressed at highly levels in MSC.

[a] miRNAs = microRNAs.
[b] MSC-exosomes = mesenchymal-stem-cell-derived exosomes.
[c] MSC = mesenchymal stem cell.
[d] MSC-CM (exo−) = mesenchymal-stem-cell-derived exosome-depleted conditioned medium.

Table 2
MicroRNA ratio of MSC-exosomes to SFB-exosomes.

miRNA[a]	Ratio MSC-exo[b]:SFB-exo[c]	MSC-exo	SFB-exo
miR-494	8.34	1313.03	157.5
*miR-601	4.52	483.09	106.88
*miR-548b-5p	3.88	54.5	14.06
*miR-1246	3.78	2923.34	773.46
*miR-607	3.40	66.89	19.69
*miR-1915-3p	3.29	175.9	30.16
*miR-187-3p	3.27	193.24	59.06
*miR-4488	3.05	822.5	270.01
miR-378d	2.85	104.05	36.56
miR-188-3p	2.81	213.06	75.94
*miR-548aa	2.80	1322.94	472.51
*miR-1469	2.77	54.5	19.69
*miR-552	2.75	131.3	47.81
*miR-520d-3p	2.64	104.05	39.38
miR-1306-3p	2.64	74.32	28.13
miR-214-3p	2.58	109.01	42.19
*miR-3154	2.51	91.66	36.56
*miR-1226-3p	2.50	126.35	50.63

[a] miRNAs = microRNAs.
[b] MSC-exo = mesenchymal-stem-cell-derived exosomes.
[c] SFB-exo = synovial-fibroblast-derived exosomes.
[*] These miRNAs are not identified in mice. Differentially contained microRNAs (at least 2.5-fold difference) are shown as the ratio of MSC-exo to SFB-exo. Values for microRNAs in MSC-exo and SFB-exo are miRNAs count (miRNAs levels).

ultracentrifugation and also in the cell lysates, but not in the supernatants (MSC-CM (exo−)) after ultracentrifugation (Fig. 1A). The size distribution of the particles in the pellets after ultracentrifugation was measured with the qNano system. The numbers and sizes of particles derived from the four different MSCs were very similar. The major peak in particle size was at 65–75 nm and the overall size distribution ranged between 60 and 200 nm (Fig. 1B). These results indicate that exosomes were isolated with this ultracentrifugation protocol.

3.2. MSC-CM and MSC-exosomes promote myogenesis and angiogenesis in vitro

The effects of MSC-conditioned medium (MSC-CM), MSC-exosome suspension in DMEM (MSC-exosome), and exosome-depleted MSC-conditioned medium (MSC-CM (exo−)) on myoblast proliferation and differentiation were analyzed in C2C12 cells. MSC-CM and MSC-exosomes significantly increased the total nuclear number and the fusion indices of the C2C12 cells compared with those of the control group and the MSC-CM (exo−) group (Fig. 2A and B). The expression of myogenic marker genes, such as *Myog*, increased for a period of 3 days during differentiation in all groups. The expression *of Myod1* and *Myog* was significantly higher in the MSC-CM and MSC-exosome groups than in the control group (Fig. 2C). In contrast, the expression of *Myod1* and *Myog* in the MSC-CM (exo−) group was not significantly different from that in the control group on all days (Fig. 2C). These results

suggest that MSC-CM and MSC-exosomes including exosomes promote both the proliferation and differentiation of C2C12 cells. To analyze the effects of MSC-CM, MSC-exosomes, and MSC-CM (exo−) on angiogenic activity in vitro, migration and tube formation assays were performed. In migration assay using HUVECs, the numbers of migrated cells increased significantly after treatment with MSC-CM, MSC-exosomes, or MSC-CM (exo−) compared with the control DMEM (Fig. 3A). The tube length in the HUVECs was significantly greater after 8 days incubation with MSC-CM or MSC-exosomes compared with control DMEM (Fig. 3B). Our in vitro studies showed that the MSC-exosomes significantly promoted myogenesis and angiogenesis.

3.3. MSC-exosomes promote muscle regeneration in a muscle injury model

To evaluate the effects of MSC-exosomes on muscle regeneration in vivo, we used the cardiotoxin muscle injury model in mice. Three days after muscle injury, the myofibers showed complete necrosis in both the control group and MSC-exosome-injected group. Seven days after muscle injury, centronucleated myofibers appeared in both the control group and the MSC-exosome group. The diameters and numbers of centronucleated myofibers were significantly higher in the MSC-exosome-injected group after 7 days than in the control group (Fig. 4A). The fibrotic area was significantly smaller in the MSC-exosome group than in the control group (Fig. 4B). The capillary density was significantly greater in the MSC-exosome group than in the control group (Fig. 4C). Our in vivo analysis in a mouse model of muscle injury showed that the injection of MSC-exosomes accelerated histological muscular regeneration, with enhanced angiogenesis and reduced fibrosis. Although our in vivo data do not clarify whether the injected MSC-exosomes were incorporated into specific cells in the muscle tissue, our in vitro and in vivo data support the hypothesis that MSC-derived exosomes promote skeletal muscle repair by accelerating myogenesis and angiogenesis.

3.4. Cytokines, growth factors, and miRNAs in MSC-exosomes

We examined cytokines (102 proteins) in MSC-exosomes, MSC-CM and MSC-CM (exo−) using Cytokine Antibody Array (data not shown). Then, the levels of picked-up protein were quantified

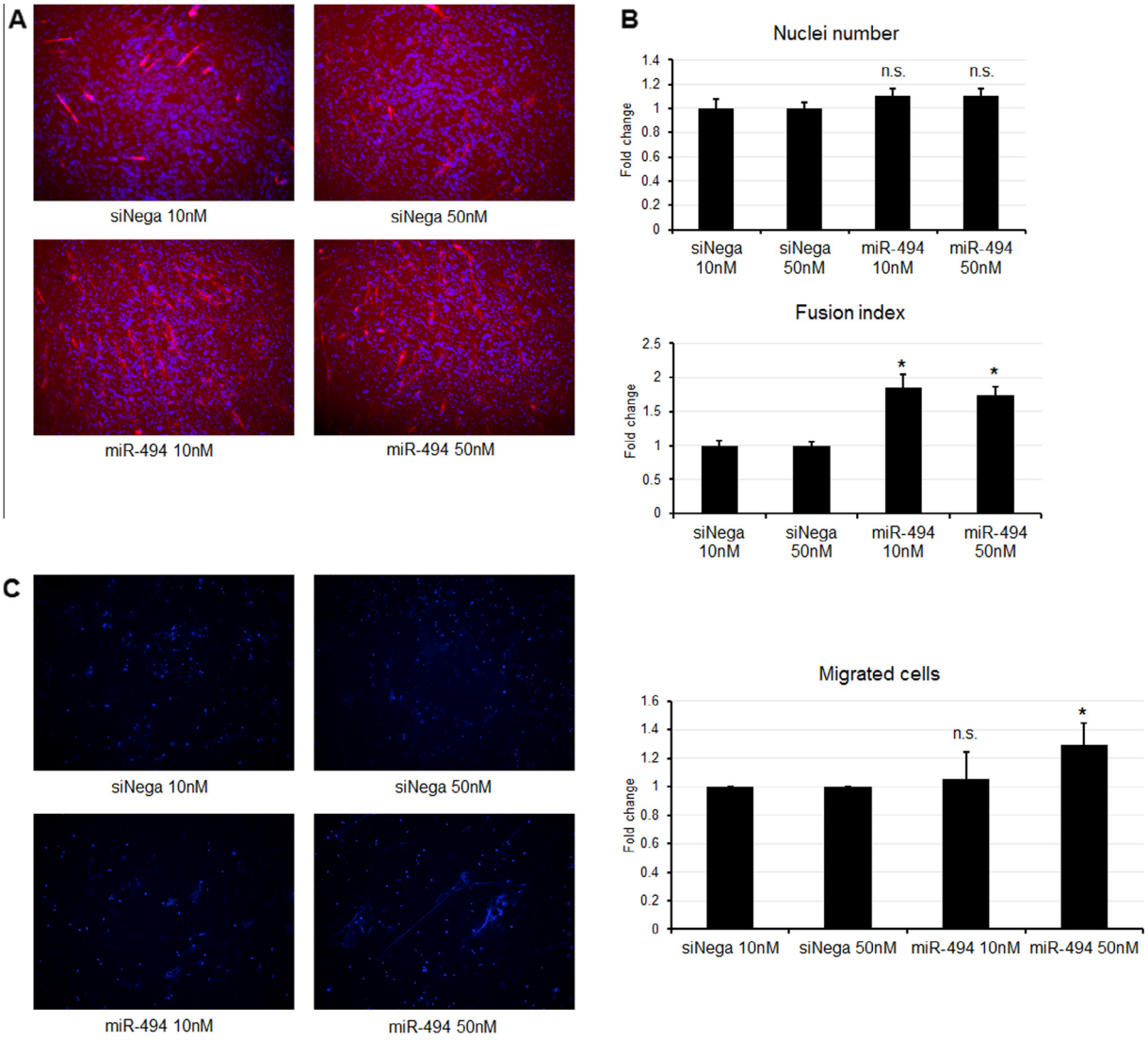

Fig. 6. Effects of miR-494 on the differentiation of C2C12 cells, the migration activity of HUVECs. (A) Myotubes are stained for myosin heavy chain (red) and nuclei are stained blue. Original magnification, ×200. (B) Total numbers of nuclei indicate myoblast proliferation. Fusion index reflects differentiation in C2C12 cells. (C) Migration assay was performed with HUVECs transfected with miR-494 or siNega. Nuclei of migrated cells are stained blue. Original magnification, ×100. All data are means ± S.E. ($n = 5$). Statistical analysis was performed with the Steel–Dwass test. *$P < 0.05$ versus siNega. Abbreviations: miR-494, microRNA-494; n.s., not significant; siNega, small interfering RNA, negative silencing control.

using ELISA and the Bio-Plex Multiplex suspension assay system. MSC-CM and MSC-CM (exo−) included significant amounts of VEGF and IL-6 which are known to be associated with skeletal muscle [23,24]. However, MSC-exosomes included significantly lower VEGF and IL-6 levels than MSC-CM or MSC-CM (exo−). The levels of FGF-2, GCSF, and PDGF-BB which are muscle-repair-related cytokines were no difference in all groups. IGF-1 was not detectable in any sample (Fig. 5). These results suggest that the paracrine effects of MSCs are not only attributable to cytokines and growth factors, but also to other factors, such as exosomes. Therefore, MSC-derived exosomes may function as a novel regulatory factor that contributes to the regeneration of skeletal muscle. This prompted us to examine miRNA in MSC-exosomes, MSC and MSC-CM (exo−) using a NanoString miRNA analysis. Among the top 20 miRNAs, miRNAs in MSC-CM (exo−) almost coincided with highly expressed miRNAs in MSC but not in the MSC-exosomes (Table 1). miR-21, an antiapoptotic miRNA [25], was detected at the highest concentrations in MSC-exosomes. Many miRNAs including miR-21 were present in both MSC-exosomes and MSC-CM (exo−). However, we reported that exosome-formed miRNAs may be more functional extracellular miRNA than non-exosome-formed miRNAs [26]. We observed that miRNAs related to tissue regeneration, such as antiapoptotic and antioxidant miRNAs, were present in the MSC-exosomes. In fact, the antiapoptotic and antioxidant effects of MSC-conditioned medium have been reported [12–14]. We also detected other myogenic miRNAs in exosomes, including miR-1, miR-133, and miR-206. The local injection of these miRNAs accelerated muscle regeneration in a rat model of skeletal muscle injury [27]. The contents of exosomes, including proteins, miRNAs, and mRNAs, vary according to the cell type that secretes them [9,10]. To focus on specific miRNAs in the MSC-exosomes, furthermore, we compared SFB-exosomes with MSC-exosomes (Table 2). Several miRNAs were identified only in exosomes and miRNAs such as miR-494 was contained abundantly in MSC-exosomes compared with SFB-exosomes. The injection of MSC-derived exosomes and the cardiac-specific overexpression of miR-494 have been reported to protect against ischemia/reperfusion-induced cardiac injury [15,16,28]. These reports suggest the miR-494 in MSC-exosomes is important in tissue repair.

3.5. miR-494 enhance myogenesis and migration activity

Recently, Yamamoto et al. showed that miR-494 was decreased in C2C12 during myogenesis, and regulated mitochondorial biogenesis via Mitochondrial transcription factor A (mtTFA) and Forkhead box j3 (FOXj3) [29]. To evaluate the effects of miR-494 on myogenesis and migration activities, C2C12 cells or HUVECs were transfected with miR-494. The numbers of nuclei in C2C12 cells transfected with miR-494 did not differ significantly from those in cells transfected with siNega. The fusion indices of C2C12 cells transfected with miR-494 were significantly higher than those of cells transfected with siNega (Fig. 6A and B). The migration activity of HUVECs transfected with miR-494 was significantly higher than that of cells transfected with siNega (Fig. 6C). Although the introduction of a single high-dose miRNA into cells may not reflect the function of that miRNA in exosomes, these results have shown that miR-494 participates in C2C12 myogenesis and HUVEC migration. Many studies have not addressed the direct effects of mediators in exosomes, such as miRNAs. The study of neurological diseases and injury has demonstrated that the transfer of miRNAs to neural cells via exosomes from MSCs contributes to neurite outgrowth [17]. Although the physiological properties of exosomes are incompletely understood, these reports support our finding that MSC-derived exosomes promote muscle regeneration at least in part via miRNAs (see Fig. 6).

Exosomes including miRNAs from MSCs may explain the mechanism of skeletal muscle regeneration during MSC transplantation, in addition to their secretion of cytokines, chemokines, or growth factors and may be a new therapeutic tool.

Acknowledgments

This project was supported by a MEXT/JSPS KAKENHI Grant-in-Aid for Scientific Research (A) Grant Number 25253089 (M.O.), young scientists (A) Grant Number 24689057 (S.M.), and the Mochida Memorial Foundation for Medical and Pharmaceutical Research (S.M.).

References

[1] Phinney, D.G. and Prockop, D.J. (2007) Concise review: mesenchymal stem/multipotent stromal cells: the state of transdifferentiation and modes of tissue repair–current views. Stem Cells 25, 2896–2902.
[2] Caplan, A.I. and Dennis, J.E. (2006) Mesenchymal stem cells as trophic mediators. J. Cell. Biochem. 98, 1076–1084.
[3] Xia, C. and Cao, J. (2013) Imaging the survival and utility of pre-differentiated allogeneic MSC in ischemic heart. Biochem. Biophys. Res. Commun. 438, 382–387.
[4] Natsu, K., Ochi, M., Mochizuki, Y., Hachisuka, H., Yanada, S. and Yasunaga, Y. (2004) Allogeneic bone marrow-derived mesenchymal stromal cells promote the regeneration of injured skeletal muscle without differentiation into myofibers. Tissue Eng. 10, 1093–1112.
[5] Gnecchi, M. et al. (2006) Evidence supporting paracrine hypothesis for Akt-modified mesenchymal stem cell-mediated cardiac protection and functional improvement. FASEB J. 20, 661–669.
[6] Kunter, U., Rong, S., Djuric, Z., Boor, P., Muller-Newen, G., Yu, D. and Floege, J. (2006) Transplanted mesenchymal stem cells accelerate glomerular healing in experimental glomerulonephritis. J. Am. Soc. Nephrol. 17, 2202–2212.
[7] Banas, A. et al. (2008) IFATS collection: in vivo therapeutic potential of human adipose tissue mesenchymal stem cells after transplantation into mice with liver injury. Stem Cells 26, 2705–2712.
[8] Ortiz, L.A., Dutreil, M., Fattman, C., Pandey, A.C., Torres, G., Go, K. and Phinney, D.G. (2007) Interleukin 1 receptor antagonist mediates the antiinflammatory and antifibrotic effect of mesenchymal stem cells during lung injury. Proc. Natl. Acad. Sci. U.S.A. 104, 11002–11007.
[9] Valadi, H., Ekstrom, K., Bossios, A., Sjostrand, M., Lee, J.J. and Lotvall, J.O. (2007) Exosome-mediated transfer of mRNAs and microRNAs is a novel mechanism of genetic exchange between cells. Nat. Cell Biol. 9, 654–659.
[10] Kosaka, N., Iguchi, H., Yoshioka, Y., Takeshita, F., Matsuki, Y. and Ochiya, T. (2010) Secretory mechanisms and intercellular transfer of microRNAs in living cells. J. Biol. Chem. 285, 17442–17452.
[11] Sabin, K. and Kikyo, N. (2013) Microvesicles as mediators of tissue regeneration. Transl. Res..
[12] Bruno, S. et al. (2009) Mesenchymal stem cell-derived microvesicles protect against acute tubular injury. J. Am. Soc. Nephrol. 20, 1053–1067.
[13] Bruno, S., Grange, C., Collino, F., Deregibus, M.C., Cantaluppi, V., Biancone, L., Tetta, C. and Camussi, G. (2012) Microvesicles derived from mesenchymal stem cells enhance survival in a lethal model of acute kidney injury. PLoS One 7, e33115.
[14] Zhou, Y. et al. (2013) Exosomes released by human umbilical cord mesenchymal stem cells protect against cisplatin-induced renal oxidative stress and apoptosis in vivo and in vitro. Stem Cell Res. Ther. 4, 34.
[15] Lai, R.C. et al. (2010) Exosome secreted by MSC reduces myocardial ischemia/reperfusion injury. Stem Cell Res. 4, 214–222.
[16] Bian, S., Zhang, L., Duan, L., Wang, X., Min, Y. and Yu, H. (2013) Extracellular vesicles derived from human bone marrow mesenchymal stem cells promote angiogenesis in a rat myocardial infarction model. J. Mol. Med. (Berl.).
[17] Xin, H. et al. (2012) Exosome-mediated transfer of miR-133b from multipotent mesenchymal stromal cells to neural cells contributes to neurite outgrowth. Stem Cells 30, 1556–1564.
[18] Xin, H., Li, Y., Cui, Y., Yang, J.J., Zhang, Z.G. and Chopp, M. (2013) Systemic administration of exosomes released from mesenchymal stromal cells promote functional recovery and neurovascular plasticity after stroke in rats. J. Cereb. Blood Flow Metab. 33, 1711–1715.
[19] Li, T. et al. (2013) Exosomes derived from human umbilical cord mesenchymal stem cells alleviate liver fibrosis. Stem Cells Dev. 22, 845–854.
[20] Zhu, Y.G. et al. (2013) Human mesenchymal stem cell microvesicles for treatment of *E. coli* endotoxin-induced acute lung injury in mice. Stem Cells.
[21] Maier, R., Ganu, V. and Lotz, M. (1993) Interleukin-11, an inducible cytokine in human articular chondrocytes and synoviocytes, stimulates the production of the tissue inhibitor of metalloproteinases. J. Biol. Chem. 268, 21527–21532.
[22] de Vrij, J. et al. (2013) Quantification of nanosized extracellular membrane vesicles with scanning ion occlusion sensing. Nanomedicine (Lond.) 8, 1443–1458.

[23] Sassoli, C. et al. (2012) Bone marrow mesenchymal stromal cells stimulate skeletal myoblast proliferation through the paracrine release of VEGF. PLoS One 7, e37512.
[24] Hoene, M., Runge, H., Haring, H.U., Schleicher, E.D. and Weigert, C. (2013) Interleukin-6 promotes myogenic differentiation of mouse skeletal muscle cells: role of the STAT3 pathway. Am. J. Physiol. Cell Physiol. 304, C128–C136.
[25] Chan, J.A., Krichevsky, A.M. and Kosik, K.S. (2005) MicroRNA-21 is an antiapoptotic factor in human glioblastoma cells. Cancer Res. 65, 6029–6033.
[26] Shimbo, K., Miyaki, S., Ishitobi, H., Kato, Y., Kubo, T., Shimose, S. and Ochi, M. (2014) Exosome-formed synthetic microRNA-143 is transferred to osteosarcoma cells and inhibits their migration. Biochem. Biophys. Res. Commun..
[27] Nakasa, T., Ishikawa, M., Shi, M., Shibuya, H., Adachi, N. and Ochi, M. (2010) Acceleration of muscle regeneration by local injection of muscle-specific microRNAs in rat skeletal muscle injury model. J. Cell Mol. Med. 14, 2495–2505.
[28] Wang, X. et al. (2010) MicroRNA-494 targeting both proapoptotic and antiapoptotic proteins protects against ischemia/reperfusion-induced cardiac injury. Circulation 122, 1308–1318.
[29] Yamamoto, H., Morino, K., Nishio, Y., Ugi, S., Yoshizaki, T., Kashiwagi, A. and Maegawa, H. (2012) MicroRNA-494 regulates mitochondrial biogenesis in skeletal muscle through mitochondrial transcription factor A and Forkhead box j3. Am. J. Physiol. Endocrinol. Metab. 303, E1419–27.